THE JOURNAL OF PHYSICAL CHEMISTRY B

Article

pubs.acs.org/JPCB

# Catalytic Mechanism of Porphobilinogen Synthase: The Chemical Step Revisited by QM/MM Calculations

Bo-Xue Tian,[†] Edvin Erdtman,[‡] and Leif A. Eriksson*[,§]

[†]School of Chemistry, National University of Ireland—Galway, Galway, Ireland

[‡]School of Engineering, University of Borås, 501 90 Borås, Sweden

[§]Department of Chemistry and Molecular Biology, University of Gothenburg, 412 96 Göteborg, Sweden

Supporting Information

**ABSTRACT:** Porphobilinogen synthase (PBGS) catalyzes the asymmetric condensation and cyclization of two 5-aminolevulinic acid (5-ALA) substrate molecules to give porphobilinogen (PBG). The chemical step of PBGS is herein revisited using QM/MM (ONIOM) calculations. Two different protonation states and several different mechanisms are considered. Previous mechanisms based on DFT-only calculations are shown unlikely to occur. According to these new calculations, the deprotonation step rather than ring closure is rate-limiting. Both the C−C bond formation first mechanism and the C−N bond formation first mechanism are possible, depending on how the A-site ALA binds to the enzyme. We furthermore propose that future work should focus on the substrate binding step rather than the enzymatic mechanism.

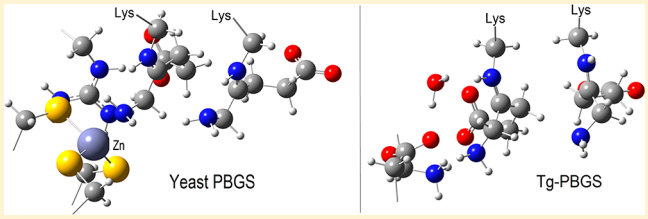


## 1. INTRODUCTION

Tetrapyrrole derivatives, such as porphyrin, chlorine, and corrin, are essential to most life forms.[1] Porphobilinogen synthase (PBGS) catalyzes the asymmetric condensation and cyclization of two 5-aminolevulinic acid (5-ALA) substrate molecules to give porphobilinogen (PBG) and is known as the first common step in the biosynthesis of the tetrapyrroles (Scheme 1).[2−4]

**Scheme 1. Reaction Catalyzed by PBGS**

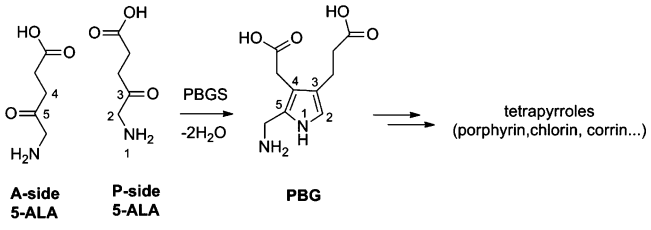


PBGSs from most organisms utilize metal ions ($Zn^{2+}$, $Mg^{2+}$, $K^{+}$, and $Na^{+}$) as cofactors. The metal ions of PBGS reside at two sites, that is, the active site and the allosteric site.[5] Most PBGSs have $Zn^{2+}$ or $Mg^{2+}$ in the active site,[5−9] albeit some do not use any active site metal ion at all.[10] PBGSs that have active site $Zn^{2+}$ are commonly found in metazoan (including human), archea, and yeast organisms. We herein focus on the yeast PBGS to illustrate the catalytic process of the enzyme (Scheme 2).

The two substrate molecules bind to the enzyme separately. To distinguish the two ALA molecules, the labels A (acetyl-) and P (propionyl-) are used throughout this study (Scheme 1), referring to the length of the resulting carboxylic acid tail in the final PBG molecule. When the active site lid is open, the P-site substrate binds to the enzyme first and forms a Schiff base with

**Scheme 2. Catalytic Process of PBGS**

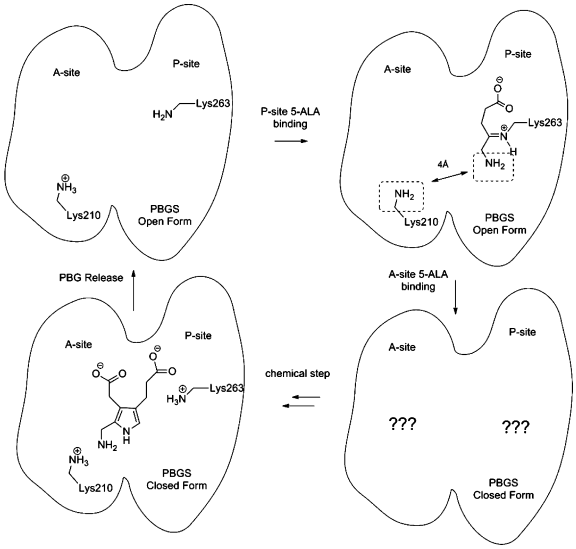


the P-site lysine (Lys263, yeast numbering; Scheme 2).[6,7,11] A water molecule is released and the second substrate enters the active site. With the A-site ALA bound, the active site lid becomes closed to prevent further solvent molecules from entering the active site.[12] Binding of the A-site ALA is controversial, as the intermediate with both substrates bound is short-lived and has never been observed.[12] Crystal structures of

**Received:** May 16, 2012
**Revised:** August 8, 2012
**Published:** September 13, 2012

   dx.doi.org/10.1021/jp304743c | J. Phys. Chem. B 2012, 116, 12105−12112

PBGS-inhibitor complexes[13−15] have shown that the A-site ALA might also form a Schiff base with the A-site lysine (Lys210). Mutagenesis studies suggest that the P-site lysine is more important than the A-site lysine in terms of decrease in enzymatic activity.[16] It is argued that the A-site ALA should bind in a geometry that will support the highly exothermic reaction and block access to the bulk solvent, irrespective of whether an A-site Schiff base is formed or not.[12]

In the current quantum mechanics/molecular mechanics (QM/MM) study, we have considered several starting structures and two different protonation states for the Michaelis complex, aiming to fill the "blank" in Scheme 2. Given the short distance between the nitrogen atom of Lys210 and that of P-site bound ALA (~4 Å in crystal structure 1H7O;[6] Scheme 2), we suggest that the A-site ALA may bind directly to the P-site ALA via Schiff base formation to get PS1-S or PS2-S (Scheme 3);

**Scheme 3. Michaelis Complexes Considered in the Current Study**

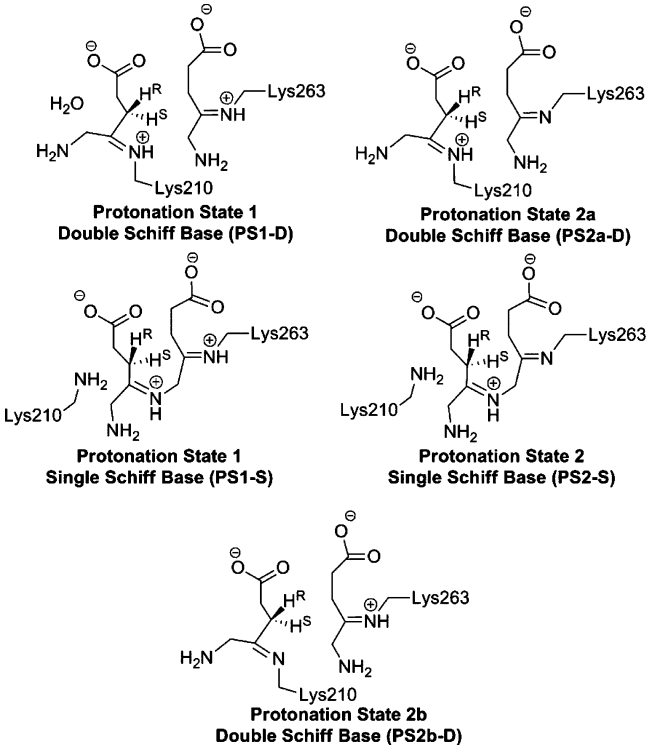


such Michaelis complexes were not considered previously (PS2-S is an intermediate in our earlier DFT study[17]). The Schiff base formation as well as Schiff base exchange reactions are not considered in this study because multiple groups (water molecules, metal ions as well as active site residues) are probably involved,[18,19] along with conformational changes of the enzyme.[12]

The role of the active site zinc ion has been discussed in a number of studies,[5,7,12,18,20−27] but no consensus has been reached. In the crystal structure of the yeast PBGS-PBG* intermediate,[7] $Zn^{2+}$ binds to three cysteine residues (Cys133, Cys135, and Cys143) as well as the amino nitrogen of the A-site ALA. It is suggested that $Zn^{2+}$ is important for facilitating the binding and reactivity of the A-site ALA, as well as maintaining the stability of the enzyme structure.[7,12,25,26] It has also been hypothesized that the active site $Zn^{2+}$ is important for removal of the hydroxyl group during the Schiff base formation and for controlling various proton transfer processes via electrostatic interactions.[18] Recently, the crystal structure of the yeast PBGS-PBG* intermediate[7] (which has an active site $Zn^{2+}$) and the crystal structure of *Toxoplasma gondii* PBGS-PBG complex[10] (Tg-PBGS, which has no active site metal ion) were resolved, which reveal that the orientation of the product, as well as the positioning of most of the conserved residues, are almost identical (Scheme 4).[10] We therefore base our models

**Scheme 4. QM Region of the QM/MM Calculations: (a) Yeast PBGS; (b) Tg-PBGS**

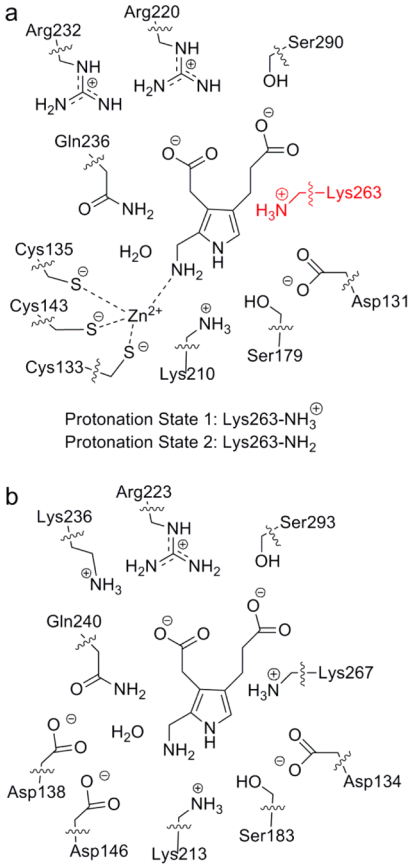


on the assumption that active site metal ion is used for binding the A-site ALA but not for the chemical step.

Another issue is how the pyrrole ring of PBG is formed.[28,29] Generally speaking, there are two routes to reach the pyrrole ring, either C3−C4 bond formation first or C5−N1 bond formation first (numbering cf. Scheme 1). Recent crystal structures[6,7,13,15] of PBGS-inhibitor complexes as well as isotope experiments[18,30] support the C3−C4 bond formation first pathway,[18] hereafter defined as Mechanism 1 (Scheme 5). In contrast, small model DFT calculations favor the C5−N1 bond formation first pathway,[17] which is defined as Mechanism 2 (Scheme 6). It should be noted that the protonation state of Mechanism 2 is different from that of Mechanism 1. The favored mechanisms might hence be different for different protonation states.[31]

In this study, various mechanisms for the chemical step are modeled using the yeast PBGS. Mechanisms 1 and 4, which we show are the most likely ones, are also modeled using the Tg-PBGS structure, to validate the assumption that the active site metal ion is not involved in the chemical step. We wish to address the following questions: (1) whether Schiff base formation of A-site ALA with A-site Lys210 is necessary for catalysis; (2) which protonation state or starting structure is


dx.doi.org/10.1021/jp304743c | J. Phys. Chem. B 2012, 116, 12105−12112

**Scheme 5. Mechanism 1**[a]

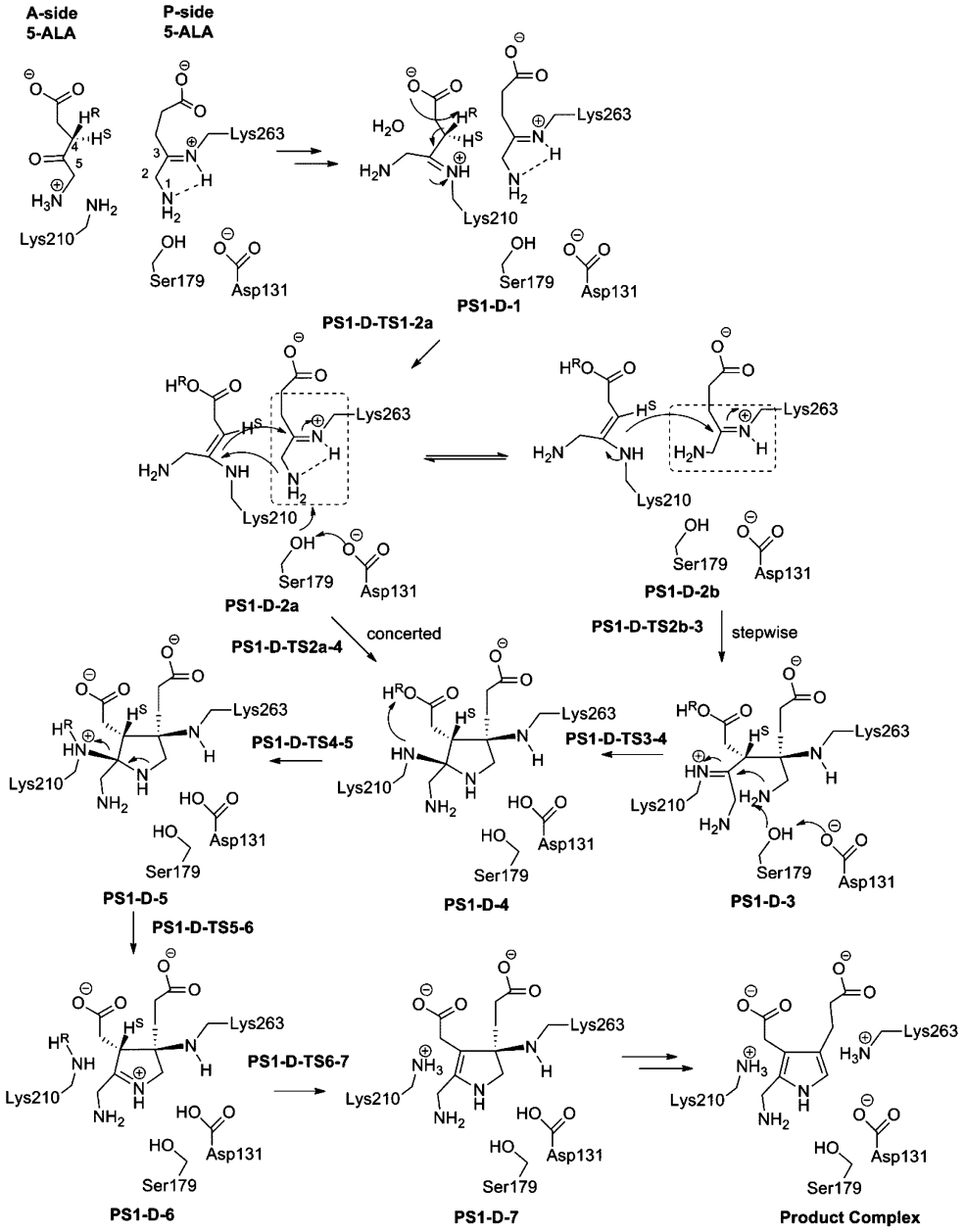


[a]Reference 18, with small modification.

preferred; (3) which bond (C3−C4 or C5−N1) is formed first in the reaction.

## 2. COMPUTATIONAL DETAILS

The crystal structures of the yeast PBGS-PBG* intermediate (PDB code 1OHL[7]) and the *Toxoplasma gondii* PBGS-PBG complex (PDB code 3OBK[10]) were obtained from the RCSB Protein Data Bank. Monomers of the two structures were used. Hydrogen atoms were added using the Molecular Operating Environment (MOE) software (version 2010.10).[32] Protonation states of the active site atoms are summarized in Scheme 4. The complex with charged Lys263 is called Protonation State 1 (protonation state used by Goodwin et al.[18]) and that with Lys263 neutral is called Protonation State 2 (protonation state used by Erdtman et al.[17]). In yeast PBGS, the three active site cysteines are set to the deprotonated form, as the Zn−S distances in the crystal structure suggest this pattern (the Zn−S distances in 1OHL are 2.33, 2.33, and 2.30 Å, respectively). If the cysteines are protonated, the Zn−S distance should be ∼2.70 Å.[33] The Zn−S distances (2.25−2.35 Å) obtained from our QM/MM optimizations are consistent with those found in the crystal structure.

The QM region in the QM/MM calculations of the two systems is described in Scheme 4. Starting from the crystal structures of the PBGS-PBG*[7] and PBGS-PBG[10] complexes, the different Michaelis complexes were traced backward. The results for the forward and reverse reactions are consistent. The systems were initially optimized using the AMBER 03 force field.[34] Missing parameters of PBG were derived using Antechamber[35,36] and the partial atomic charges were assigned using the RESP charge method (Supporting Information, S1). QM/MM methods have been extensively used for modeling enzymatic


dx.doi.org/10.1021/jp304743c | J. Phys. Chem. B 2012, 116, 12105−12112

**Scheme 6. Mechanisms 2 and 3**[a]

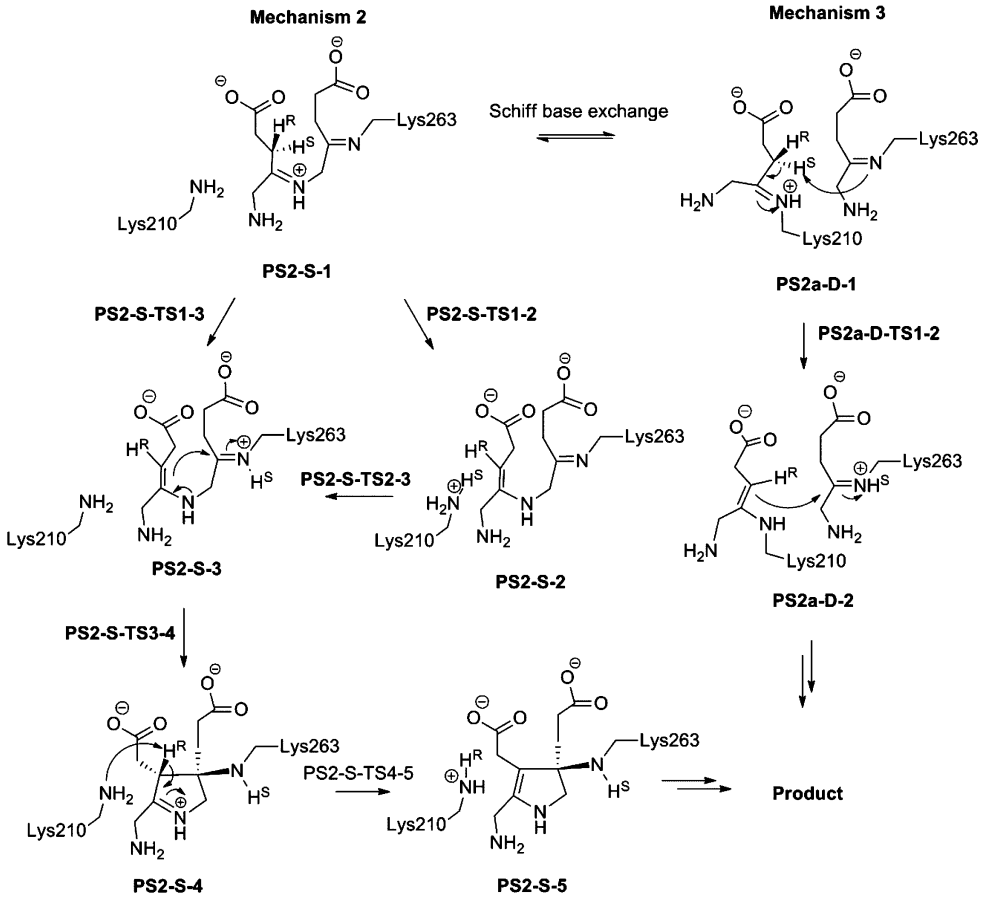


[a]Reference 17, with small modification.

reactions;[37−39] we have herein used a two-layer ONIOM (QM/MM) scheme[40] with electronic embedding (EE). Geometries were optimized with the ONIOM-EE (B3LYP/[41−43]AMBER) method. The SDD basis set[44] was used for $Zn^{2+}$ and 6-31G(d) for the other atoms (Table 1), a combination that has been successfully employed in a number of QM/MM studies on zinc-containing enzymes.[45−49] Atoms far away from the PBG atoms (>10 Å) were held fixed during the QM/MM optimizations. Frequency calculations were performed on the QM atoms only (using the "geom.= readfreeze" option in G09) to confirm the correct normal modes of the imaginary frequency in those TSs. Full frequency calculations were not performed due to shortage of memory. Single-point energy calculations were performed on the optimized geometries with a larger basis set (see Table 1 for details). All the ONIOM calculations were performed using the Gaussian 09 software.[50]

**Table 1. Summary of Computational Details**

| | yeast PBGS | Tg-PBGS |
|---|---|---|
| protonation state | PS1 and PS2 | PS1 |
| mechanism studied | all mechanisms | Mechanisms 1 and 4 |
| geometry optimization | B3LYP/BS1/AMBER[a] | B3LYP/BS3/AMBER[c] |
| single point energy | B3LYP/BS2/AMBER[b] | B3LYP/BS4/AMBER[d] |

[a]BS1: SDD for $Zn^{2+}$, 6-31G(d) for other elements. [b]BS2: SDD for $Zn^{2+}$, 6-311+G(2d,p) for other elements. [c]BS3: 6-31G(d). [d]BS4: 6-311+G(2d,p).

## 3. RESULT AND DISCUSSION

**Overview.** For the yeast PBGS system, two different protonation states are used (Scheme 4) and several different mechanisms considered. The most likely mechanisms obtained, that is, Mechanisms 1 and 4, are further modeled in the Tg-PBGS. As a lot of intermediates and transition states (TS) are involved, we divide each pathway into three stages, that is, (1) deprotonation of A-site ALA, (2) ring closure, and (3) post PBG formation steps. In the main text, we report relative energies for the key intermediates; detailed energies and geometries can be found in the Supporting Information.

**Mechanism 1.** To date, Mechanism 1 is the most favored one for PBGS.[6,7,13,15,18] According to this mechanism, both ALA molecules bind to the enzyme in the protonated Schiff base form (PS1-D-1 in Scheme 5). $H^R$ at the A-site ALA is abstracted by its own carboxyl group to give the enamine intermediate (PS1-D-2), followed by C3−C4 bond formation. Isotope effect experiments[18] show that deuterium substitution of $H^R$ has a larger isotope effect on $V_{max}$ than what $H^S$ has, but the effect on $V_{max}/K_M$ is identical for deuterium substitution at both $H^R$ and $H^S$, which suggests that deprotonation might not be the rate-limiting step.[18] PS1-D-3 is unstable and converts to the ring-closed intermediate PS1-D-4.[15] The steps from PS1-D-4 to the final product are relatively easy. According to our QM/MM calculations, a minor change to the previous mechanism is observed, in that Asp131/Ser179 can abstract a proton from the N1 atom of the P-site ALA and stabilize PS1-D-4, which was not considered previously.


dx.doi.org/10.1021/jp304743c | J. Phys. Chem. B 2012, 116, 12105−12112

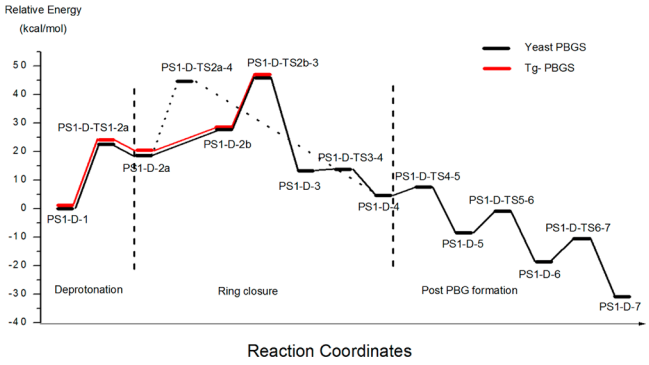


**Figure 1.** Relative energies of key intermediates and transition states in Mechanism 1.

The energies for the three stages of Mechanism 1 are summarized in Figure 1. Our results indicate that the overall rate-limiting step is the deprotonation stage, which has a barrier of 22.8 kcal/mol. The geometry of PS1-D-TS1-2a (yeast system) is shown in Figure 2. This is somewhat higher than the

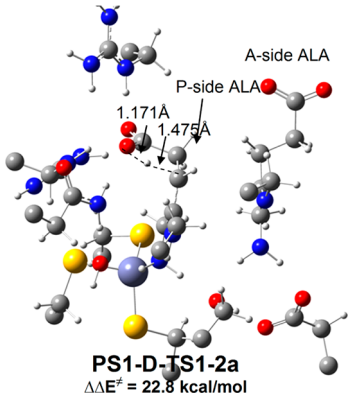


**Figure 2.** Optimized geometry of PS1-D-TS1-2a (yeast PBGS).

phenomenological barrier height of ~18 kcal/mol, derived from the experimental turnover rate[30] using the Eyring equation. The difference between theoretical results and experimental data might be due to the neglect of entropic contributions and quantum tunneling effects. In addition, deprotonation might occur in the substrate binding process and directly give the deprotonated intermediates.[12,18] As the geometries are only optimized locally (cf. Computational Details), the transition from the open form to the closed form or other large conformational changes are also not considered in this work.

The ring closure stage can start from two different conformations, PS1-D-2a and PS1-D-2b (Figure 3). The difference between these is whether the Schiff base proton of Lys263 forms a hydrogen bond with the N1 atom (Figure 3 and Scheme 5) or not. This hydrogen bond stabilizes PS1-D-2a and increases the barrier height for the C3−C4 bond formation ($\Delta E^{\ddagger}$ = 25.5 kcal/mol in PS1-D-2a vs $\Delta E^{\ddagger}$ = 19.0 kcal/mol in PS1-D-2b). Interestingly, the conversion PS1-D-2a → PS1-D-4 is concerted (Supporting Information, S2). Although intermediate PS1-D-3 can be found in the stepwise pathway from PS1-D-2b (Scheme 5), the conversion PS1-D-3 → PS1-D-4 is barrierless (Figure 1), implying that PS1-D-3 is unstable. As the stepwise ring closure from PS1-D-2b ($\Delta E^{\ddagger}$ = 19.0 kcal/mol, Figure 4) is more favorable than the concerted ring closure from PS1-D-2a ($\Delta E^{\ddagger}$ = 25.5 kcal/mol), we suggest that before

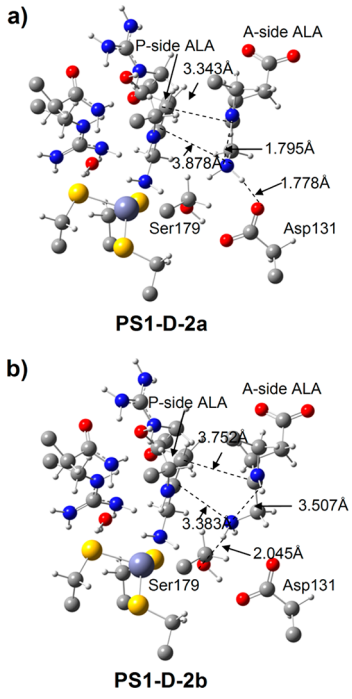


**Figure 3.** Optimized geometries of (a) PS1-D-2a and (b) PS1-D-2b (yeast PBGS).

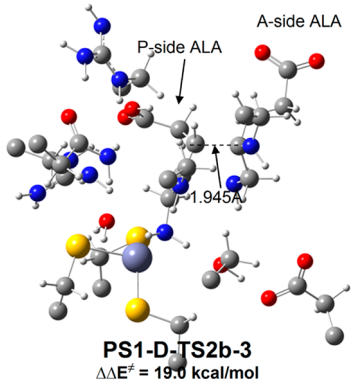


**Figure 4.** Optimized geometry of PS1-D-TS2b-3 (yeast PBGS).

the C3−C4 bond formation, PS1-D-2a must convert to PS1-D-2b by breaking the hydrogen bond between N1 and the iminium proton of Lys263 through a rotation of the N−C3−C2−N1 dihedral angle. The PBG formation stage is fast and we did not observe any step that has a barrier height of more than 10 kcal/mol (Figure 1). The key conversions PS1-D-1 → PS1-D-2a and PS1-D-2b → PS1-D-3 are also modeled in the Tg-PBGS system, and the results are consistent with those in the yeast PBGS system. This suggests that the active site metal ion is presumably not involved in the chemical step.

**Mechanisms 2 and 3.** Mechanisms 2 and 3 were previously studied using DFT-only (B3LYP/6-31G(d)//IEFPCM) calculations, and Mechanism 2 was shown to be more favorable than Mechanism 3.[17] However, in our QM/MM calculations on the PS2 system (Scheme 6), the barrier heights for deprotonation are dramatically different from the DFT-only calculations. It should be noted that the protonation state PS2 is used in both Mechanism 2 and Mechanism 3, albeit there is strong experimental evidence that the P-site Schiff base is protonated when the first ALA (P-site ALA) binds (Scheme 2).[11]


dx.doi.org/10.1021/jp304743c | J. Phys. Chem. B 2012, 116, 12105−12112

**Table 2. Relative Energies of Key Intermediates and Transition States in Mechanism 2**

| stage | intermediate or TS | relative energy[a] |
|---|---|---|
| deprotonation | PS2-S-1 | 0.0 |
| | PS2-S-TS1-2 | 30.0 |
| | PS2-S-2 | 6.4 |
| | PS2-S-TS2-3 | 16.3 |
| | PS2-S-TS1-3 | 37.5 |
| ring closure | PS2-S-3 | 7.5 |
| | PS2-S-TS3-4 | 23.0 |
| post PBG formation | PS2-S-4 | −8.1 |
| | PS2-S-TS4-5 | 1.4 |
| | PS2-S-5 | −22.3 |

[a]ONIOM(B3LYP/BS2:AMBER)//ONIOM(B3LYP/BS1:AMBER) energies, yeast PBGS system, in kcal/mol.

**Table 3. Relative Energies of Key Intermediates and Transition States in Mechanism 3**

| stage | intermediate or TS | relative energy[a] |
|---|---|---|
| deprotonation | PS2a-D-1 | 0.0 |
| | PS2a-D-TS1−2 | 42.0 |
| ring closure | PS2a-D-2[b] | −13.3 |
| | PS2a-D-TS2−3 | 3.6 |

[a]ONIOM(B3LYP/BS2/AMBER)//ONIOM(B3LYP/BS1/AMBER) energies, yeast PBGS system, in kcal/mol. [b]Conformation similar to PS1-D-2b is used.

**Scheme 7. Mechanism 4**

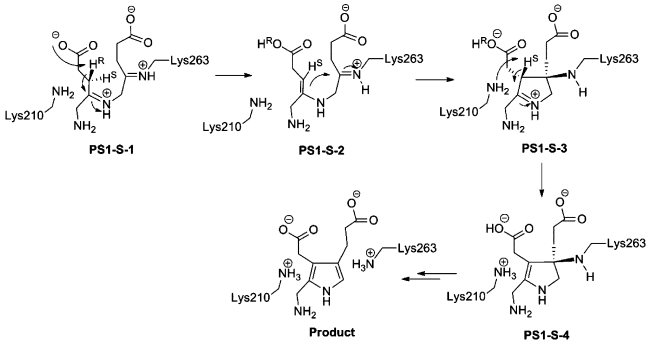


In the previous B3LYP/6-31G(d)//IEFPCM calculations, the barrier heights for conversions PS2-S-1→ PS2-S-3 and PS2-D-1 → PS2-D-2 were 12.1 and 19.4 kcal/mol, respectively. However, in the current ONIOM calculations, the barrier heights for these two steps are considerably higher, 37.5 and 42.0 kcal/mol, suggesting that such conversions are unlikely to occur in PBGS. Such large differences between QM and QM/MM calculations may be due to the easier rotation of the N═C double bond in the Lys263 imine group (the nitrogen then abstracts the C4 proton $H^S$) in the QM-only calculations, which have more degrees of freedom. In addition, the overall electrostatic effects may also influence the barriers of these two conversions. An alternative pathway is also considered, in which Lys210 acts as a proton shuttle (Scheme 6), but the barrier height is still very high (PS2-S-TS1−2, $\Delta E^{\ddagger}$ = 30.0 kcal/mol). We therefore suggest that the mechanisms in the DFT-only calculations[17] might be problematic and that neglecting the enzymatic environment is not suitable for modeling these enzymatic reactions. Interestingly, the barriers for the subsequent

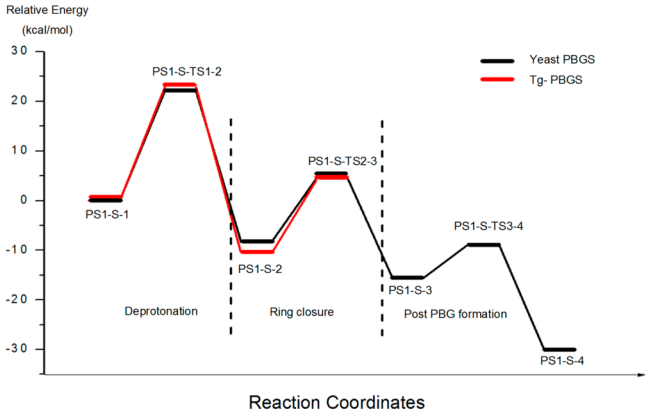


**Figure 5.** Relative energies of key intermediates and transition states in Mechanism 4.

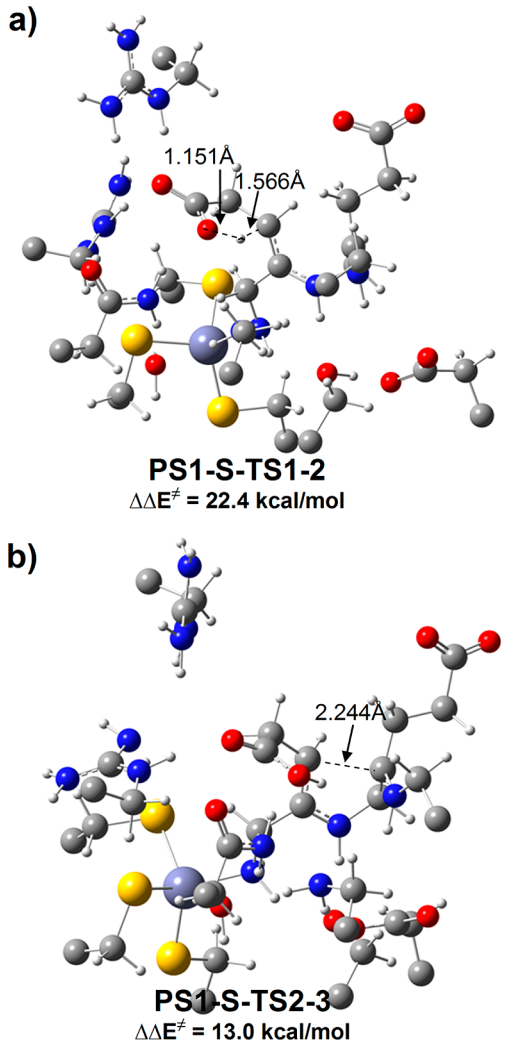


**Figure 6.** Optimized geometries of (a) PS1-S-TS1-2 and (b) PS1-S-TS2-3 (yeast PBGS).

ring closure stage are actually not high (15.5 and 16.9 kcal/mol, respectively), and if there is some other pathway that gives PS2-S-3 or PS2a-D-2, the ring closure should be straightforward (Tables 2 and 3).

**Mechanism 4.** Mechanism 4 is similar to Mechanism 2, with the main variation that the P-site Schiff base is now


dx.doi.org/10.1021/jp304743c | J. Phys. Chem. B 2012, 116, 12105−12112

Scheme 8. Base Groups That Can Abstract the C4 Protons

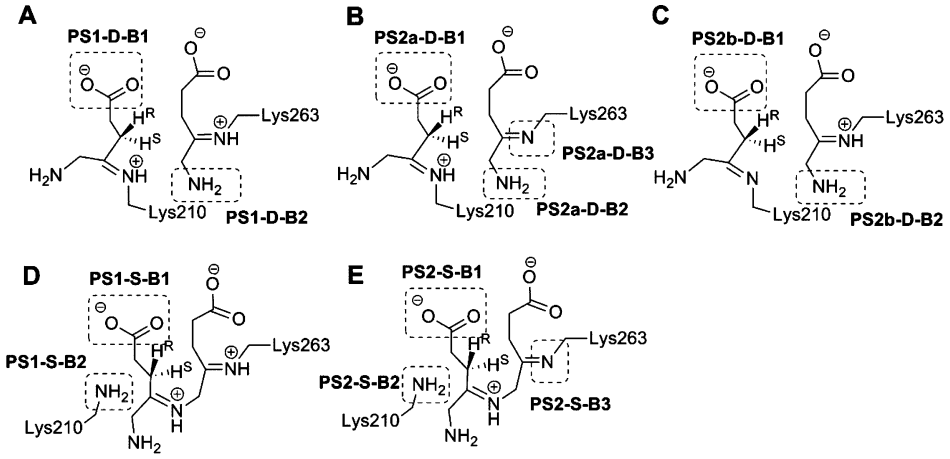


Table 4. Summary of Energy Barriers for Deprotonation

| | | deprotonation barrier[b] | |
|---|---|---|---|
| | base group[a] | $H^R$ | $H^S$ |
| A | PS1-D-B1 | 22.8 | |
| | PS1-D-B2 | | 29.0 |
| B | PS2a-D-B1 | 31.1 | |
| | PS2a-D-B2 | | 36.8 |
| | PS2a-D-B3 | | 42.0 |
| C | PS2b-D-B1 | 45.7 | |
| | PS2b-D-B2 | | 48.0 |
| D | PS1-S-B1 | 22.4 | |
| | PS1-S-B2 | 25.6 | 28.8 |
| E | PS2-S-B1 | 37.5 | |
| | PS2-S-B2 | 26.1 | 30.0 |
| | PS2-S-B3 | | 46.5 |

[a]Base groups are defined in Scheme 8. [b]ONIOM(B3LYP/BS2/AMBER)//ONIOM(B3LYP/BS1/AMBER) energies, in kcal/mol.

protonated (Scheme 7). Although deprotonation in Mechanism 4 is still as difficult as in Mechanism 1 (22.4 kcal/mol vs 22.8 kcal/mol), the ring closure becomes much easier (13.0 kcal/mol vs 19.0 kcal/mol; Figure 5). The geometries of PS1-S-TS1−2 and PS1-S-TS2−3 are shown in Figure 6. Given only 0.4 kcal/mol difference for the rate-limiting step, we suggest that both Mechanism 1 (C3−C4 bond formation first) and Mechanism 4 (C5−N1 bond formation first) are possible. It should be noted that the K210A mutation causes 1000-fold decrease in PBGS activity; however, this mutation also significantly affects the Schiff base formation of P-site ALA.[16] Therefore, mutagenesis is unlikely to tell whether Mechanism 1 or 4 is actually the preferred one. We propose that whether Mechanism 1 or 4 occurs in PBGS is determined by the binding mode of the A-site ALA, which might be different in different PBGS enzymes.

**Other Pathways and General Consideration of the PBGS Mechanism.** Besides the four mechanisms discussed above, we also modeled other possible pathways, for example, using PS2b-D as starting structure (Schemes 3 and 8). The common feature of all the mechanisms is that the deprotonation of A-site ALA is rate-limiting. Once a deprotonated intermediate is generated, the ring closure is straightforward ($\Delta E^{\ddagger}$ = 15−19 kcal/mol in the various mechanisms). However, in all our attempts to find alternative mechanisms for PBGS, the rate-limiting (deprotonation stage) barriers are always higher than those of Mechanisms 1 and 4 (Table 4). It seems that none of the base groups (Scheme 8) considered in the current study are strong enough to abstract the C4 protons on A-site ALA (Table 4). Even in Mechanisms 1 and 4, the activation energy ∼22 kcal/mol is relatively high for an enzymatic reaction. Therefore, we suggest that future work should focus on the binding mode of A-site ALA and the deprotonation of the C4 protons, rather than which bond (C3−C4 or C5−N1) is formed first in the chemical step.

## 4. CONCLUSIONS

The chemical step of PBGS is studied. Extensive and systematic QM/MM calculations are performed on the yeast PBGS and Tg-PBGS using different Michaelis complexes. We propose that A-site ALA can form a Schiff base with either the A-site lysine or the P-site ALA, and that the Schiff base between A-site ALA and A-site lysine might not be necessary for the ring closure. Our calculations show that Mechanisms 1 and 4 are the most likely ones among all tested. Mechanism 2, which is favored in DFT-only calculations, is shown unlikely to occur. According to our calculations, the preferred protonation state is protonation state 1 in which both Schiff base nitrogens are protonated. The question whether C3−C4 or C5−N1 forms first in the reaction might be system-dependent, given that two competing mechanisms (Mechanisms 1 and 4) exist and that the ring closure stage is presumably not rate-limiting. The rate-limiting barrier of ∼22 kcal/mol for Mechanisms 1 and 4 is higher than that obtained from experimental data ∼18 kcal/mol, and possible explanations are that neither entropic nor quantum tunneling effects are considered in this work, and that deprotonation of the A-site ALA might occur already in the substrate binding process where large conformational changes are involved. Unfortunately, the current methodology is not able to evaluate such changes. MD simulations may be employed to study the conformational changes induced by the binding of A-site ALA, but are obviously nontrivial. To better understand the PBGS mechanism, we propose that future focus should be on the binding process of A-site ALA and the deprotonation of the C4 protons.

## ■ ASSOCIATED CONTENT

### Supporting Information

S1: AMBER parameters for PBG; S2: 3D relative energy surface near PS1-D-TS2a-4; S3: Complete citation for ref 50; S4: Cartesian coordinates (QM region) and QM/MM energies

of key intermediates and TSs. This material is available free of charge via the Internet at http://pubs.acs.org.

## AUTHOR INFORMATION

### Corresponding Author

*E-mail: leif.eriksson@chem.gu.se.

### Notes

The authors declare no competing financial interest.

## ACKNOWLEDGMENTS

The National University of Ireland—Galway and the Faculty of Science of the University of Gothenburg are gratefully acknowledged for financial support. The SFI/HEA Irish Centre for High-End Computing (ICHEC) is acknowledged for the provision of computational facilities and support.

## REFERENCES

(1) Battersby, A. R. *Nat. Prod. Rep.* **2000**, *17*, 507−526.
(2) Layer, G.; Reichelt, J.; Jahn, D.; Heinz, D. W. *Protein Sci.* **2010**, *19*, 1137−1161.
(3) Jordan, P. M. *Biosynthesis of Tetrapyrroles*; Elsevier: Amsterdam, 1991; Vol. *19*.
(4) Shemin, D.; Russell, C. S. *J. Am. Chem. Soc.* **1953**, *75*, 4873−4874.
(5) Jaffe, E. K. *Chem. Biol.* **2003**, *10*, 25−34.
(6) Erskine, P. T.; Newbold, R.; Brindley, A. A.; Wood, S. P.; Jordan, P. M.; Warren, M. J.; Cooper, J. B. *J. Mol. Biol.* **2001**, *312*, 133−141.
(7) Erskine, P. T.; Coates, L.; Butler, D.; Youell, J. H.; Brindley, A. A.; Wood, S. P.; Warren, M. J.; Jordan, P. M.; Cooper, J. B. *Biochem. J.* **2003**, *373*, 733−738.
(8) Kervinen, J.; Jaffe, E. K.; Stauffer, F.; Neier, R.; Wlodawer, A.; Zdanov, A. *Biochemistry* **2001**, *40*, 8227−8236.
(9) Mitchell, L. W.; Jaffe, E. K. *FASEB J.* **1992**, *6*, A459−A459.
(10) Jaffe, E. K.; Shanmugam, D.; Gardberg, A.; Dieterich, S.; Sankaran, B.; Stewart, L. J.; Myler, P. J.; Roos, D. S. *J. Biol. Chem.* **2011**, *286*, 15298−15307.
(11) Jaffe, E. K.; Markham, G. D.; Rajagopalan, J. S. *Biochemistry* **1990**, *29*, 8345−8350.
(12) Jaffe, E. K. *Bioorg. Chem.* **2004**, *32*, 316−325.
(13) Erskine, P. T.; Coates, L.; Newbold, R.; Brindley, A. A.; Stauffer, F.; Wood, S. P.; Warren, M. J.; Cooper, J. B.; Jordan, P. M.; Neier, R. *FEBS Lett.* **2001**, *503*, 196−200.
(14) Frere, F.; Schubert, W. D.; Stauffer, F.; Frankenberg, N.; Neier, R.; Jahn, D.; Heinz, D. W. *J. Mol. Biol.* **2002**, *320*, 237−247.
(15) Frere, F.; Nentwich, M.; Gacond, S.; Heinz, D. W.; Neier, R.; Frankenberg-Dinkel, N. *Biochemistry* **2006**, *45*, 8243−8253.
(16) Jordan, P. M.; Spencer, P.; Sarwar, M.; Erskine, P. E.; Cheung, K. M.; Cooper, J. B.; Norton, E. B. *Biochem. Soc. Trans.* **2002**, *30*, 584−590.
(17) Erdtman, E.; Bushnell, E. A. C.; Gauld, J. W.; Eriksson, L. A. *J. Phys. Chem. B* **2010**, *114*, 16860−16870.
(18) Goodwin, C. E.; Leeper, F. J. *Org. Biomol. Chem.* **2003**, *1*, 1443−1446.
(19) Erdtman, E.; Bushnell, E. A. C.; Gauld, J. W.; Eriksson, L. A. *Comput. Theor. Chem.* **2011**, *963*, 479−489.
(20) Barnard, G. F.; Itoh, R.; Hohberger, L. H.; Shemin, D. *J. Biol. Chem.* **1977**, *252*, 8965−8974.
(21) Bevan, D. R.; Bodlaender, P.; Shemin, D. *J. Biol. Chem.* **1980**, *255*, 2030−2035.
(22) Gibbs, P. N. B.; Gore, M. G.; Jordan, P. M. *Biochem. J.* **1985**, *225*, 573−580.
(23) Mitchell, L. W.; Volin, M.; Jaffe, E. K. *FASEB J.* **1994**, *8*, A1366−A1366.
(24) Jaffe, E. K. *Acta Crystallogr., Sect. D: Biol. Crystallogr.* **2000**, *56*, 115−128.
(25) Jaffe, E. K.; Hanes, D. *J. Biol. Chem.* **1986**, *261*, 9348−9353.
(26) Jaffe, E. K.; Martins, J.; Li, J.; Kervinen, J.; Dunbrack, R. L. *J. Biol. Chem.* **2001**, *276*, 1531−1537.
(27) Erskine, P. T.; Coates, L.; Newbold, R.; Brindley, A. A.; Stauffer, F.; Beaven, G. D. E.; Gill, R.; Coker, A.; Wood, S. P.; Warren, M. J.; Jordan, P. M.; Neier, R.; Cooper, J. B. *Acta Crystallogr., Sect. D: Biol. Crystallogr.* **2005**, *61*, 1222−1226.
(28) Jordan, P. M.; Seehra, J. S. *J. Chem. Soc., Chem. Commun.* **1980**, 240−242.
(29) Jarret, C.; Stauffer, F.; Henz, M. E.; Marty, M.; Luond, R. M.; Bobalova, J.; Schurmann, P.; Neier, R. *Chem. Biol.* **2000**, *7*, 185−196.
(30) Appleton, D.; Leeper, F. J. *Bioorg. Med. Chem. Lett.* **1996**, *6*, 1191−1194.
(31) Ferrer, S.; Silla, E.; Tunon, I.; Oliva, M.; Moliner, V.; Williams, I. H. *Chem. Commun.* **2005**, 5873−5875.
(32) MOE; Chemical Computing Group Inc.: Montreal, http://www.chemcomp.com.
(33) Dudev, T.; Lim, C. *J. Am. Chem. Soc.* **2002**, *124*, 6759−6766.
(34) Duan, Y.; Wu, C.; Chowdhury, S.; Lee, M. C.; Xiong, G. M.; Zhang, W.; Yang, R.; Cieplak, P.; Luo, R.; Lee, T.; Caldwell, J.; Wang, J. M.; Kollman, P. *J. Comput. Chem.* **2003**, *24*, 1999−2012.
(35) Wang, J. M.; Wolf, R. M.; Caldwell, J. W.; Kollman, P. A.; Case, D. A. *J. Comput. Chem.* **2004**, *25*, 1157−1174.
(36) Wang, J. M.; Wang, W.; Kollman, P. A.; Case, D. A. *J. Mol. Graph.* **2006**, *25*, 247−260.
(37) Shaik, S.; Cohen, S.; Wang, Y.; Chen, H.; Kumar, D.; Thiel, W. *Chem. Rev.* **2010**, *110*, 949−1017.
(38) Senn, H. M.; Thiel, W. *Curr. Opin. Chem. Biol.* **2007**, *11*, 182−187.
(39) Garcia-Viloca, M.; Gao, J.; Karplus, M.; Truhlar, D. G. *Science* **2004**, *303*, 186−195.
(40) Vreven, T.; Byun, K. S.; Komaromi, I.; Dapprich, S.; Montgomery, J. A.; Morokuma, K.; Frisch, M. J. *J. Chem. Theory Comput.* **2006**, *2*, 815−826.
(41) Becke, A. D. *J. Chem. Phys.* **1993**, *98*, 5648−5652.
(42) Lee, C. T.; Yang, W. T.; Parr, R. G. *Phys. Rev. B* **1988**, *37*, 785−789.
(43) Becke, A. D. *Phys. Rev. A* **1988**, *38*, 3098−3100.
(44) Dolg, M.; Wedig, U.; Stoll, H.; Preuss, H. *J. Chem. Phys.* **1987**, *86*, 866−872.
(45) Wu, R. B.; Wang, S. L.; Zhou, N. J.; Cao, Z. X.; Zhang, Y. K. *J. Am. Chem. Soc.* **2010**, *132*, 9471−9479.
(46) Wu, R. B.; Hu, P.; Wang, S. L.; Cao, Z. X.; Zhang, Y. K. *J. Chem. Theory Comput.* **2010**, *6*, 337−343.
(47) Sousa, S. F.; Fernandes, P. A.; Ramos, M. J. *J. Am. Chem. Soc.* **2007**, *129*, 1378−1385.
(48) Sousa, S. F.; Fernandes, P. A.; Ramos, M. J. *Proteins* **2007**, *66*, 205−218.
(49) Sousa, S. F.; Fernandes, P. A.; Ramos, M. J. *Biophys. J.* **2005**, *88*, 483−494.
(50) Frisch, M. J.; Trucks, G. W.; Schlegel, H. B.; Scuseria, G. E.; Robb, M. A.; Cheeseman, J. R.; Scalmani, G.; Barone, V.; Mennucci, B.; Petersson, G. A.; et al. *Gaussian 09*, Revision B.01; Gaussian, Inc.: Wallingford, CT, 2009 (for the complete citation, see Supporting Information).